GRB990123: Multiwavelength afterglow study(*)

E. Maiorano[1][2](**), N. Masetti[1], E. Palazzi[1], F. Frontera[1][3]
P. Grandi[1], E. Pian[4], L. Amati[1], L. Nicastro[5], P. Soffitta[6]
A. Corsi[6], L. Piro[6], L. A. Antonelli[7], E. Costa[6], M. Feroci[6]
J. Heise[8] and J. J. M. in 't Zand[8]

[1] *Istituto di Astrofisica Spaziale e Fisica Cosmica – (INAF) Sez. di Bologna, Italy*
[2] *Dipartimento di Astronomia, Università di Bologna, Italy*
[3] *Dipartimento di Fisica, Università di Ferrara, Italy*
[4] *Osservatorio Astronomico di Trieste – (INAF), Italy*
[5] *Istituto di Astrofisica Spaziale e Fisica Cosmica – (INAF) Sez. di Palermo, Italy*
[6] *Istituto di Astrofisica Spaziale e Fisica Cosmica – (INAF) Sez. di Roma, Italy*
[7] *Osservatorio Astronomico di Roma – (INAF) Monte Porzio Catone, Italy*
[8] *SRON, Sorbonnelaan 2, NL-3584 CA Utrecht, The Netherlands*

Summary. — We report on the *BeppoSAX* and multiwavelength data analysis of the afterglow of Gamma-Ray Burst (GRB) 990123. Mainly due to its exceptional brightness, this is the only source for which the Wide Field Cameras have allowed an early detection of the X-ray afterglow between ∼20 and 60 min after the GRB trigger. Besides, again for the first time, high-energy emission from the afterglow was detected up to 60 keV. The backwards extrapolation of the afterglow decay smoothly reconnects with the late GRB emission, thus indicating that both are consistent with being produced by the same phenomenon. For the X-ray afterglow we found a power law decay with index $\alpha_{\rm X} = 1.46 \pm 0.04$; the spectrum has a power law shape with photon index $\Gamma \sim 2$. An extensive set of multiwavelength observations on the afterglow, collected from the literature and made during the *BeppoSAX* pointing, allowed constructing a Spectral Flux Distribution. We performed an analysis of the GRB afterglow emission in the context of the "fireball" model.

PACS 95.75.Fg – Spectroscopy and spectrophotometry.
PACS 95.85.Nv – X-ray.
PACS 98.70.Rz – γ-ray sources; γ-ray bursts.
PACS 01.30.Cc – Conference proceedings.

1. – Introduction

The Gamma-Ray Burst (GRB) 990123 triggered the *BeppoSAX* [4] Gamma Ray Burst Monitor (GRBM) on 1999 January 23.4078 UT [14] and was simultaneously detected near the center of the field of view in Wide Field Camera (WFC) no. 1 [11], with a localization uncertainty of 2′ (error circle radius) at coordinates $(J2000)RA = 15^{\rm h}$
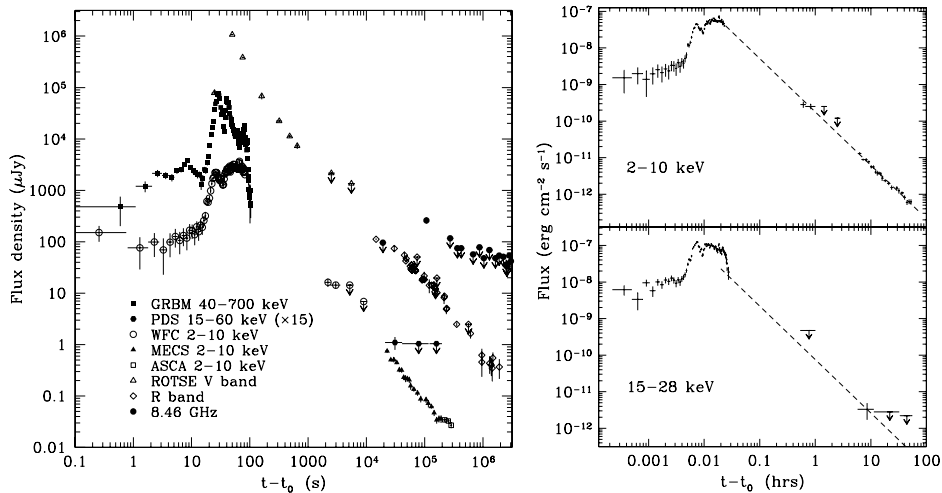
Fig. 1. – Left panel: multiwavelength light curves; t_0 corresponds to the time of the GRB onset. Right panel: 2–10 keV and 15–28 keV light curves from the prompt event to the afterglow. The dashed line is the best-fit decay obtained fron the X-ray afterglow data.

$25^m\ 29^s\!.00$, DEC $= +44°\ 45'\ 00''\!.5$ [8]. The prompt emission [6] lasted about 100 s in 40–700 keV and showed two major peaks (fig. 1, left panel). At the lower (2–10 keV) energies in the WFC data, atmospheric absorption played an important role, as it affected substantially the soft–X-ray measurements close to the end of the observation. In this burst for the first time the optical flash was observed by the Robotic Optical Transient Search Experiment (ROTSE), the OT peaked at magnitude $V \sim 9$ about 50 s after the GRB onset. The afterglow optical spectrum showed an absorbtion system at redshift $z = 1600$ [12, 2].

Here we present the data on the X-ray and multiwavelength afterglow of GRB990123. A more extensive treatment of the data presented here can be found in Maiorano *et al.* [13]. When not otherwise indicated, errors for X-ray spectral parameters will be reported at 90% confidence level ($\Delta\chi^2 = 2.7$ for one parameter fit), while errors for other parameters will be at 1σ; upper limits will be given at 3σ.

2. – Observations and data analysis

Two *BeppoSAX* Narrow-Field Instruments (NFI) observations were carried out in Target of Opportunity (ToO) mode. The observations started $\sim$ 6 h after the trigger and continued during the two following days (see table I). A fading X-ray source inside the WFC error box was detected almost at the center of the LECS and MECS detectors and it was identified as the X-ray afterglow of GRB990123 [15]. Afterglow spectra and light curves for the NFI data were then accumulated and extracted.

3. – Results

3˙1. *Light curves*. – In fig. 1 (left panel) γ-ray (40–700 keV), X-ray (2–10 keV), optical V-band [1], optical R-band [5,10,12,9], and radio (36 mm, [12]) light curves of the prompt burst and afterglow of GRB990123 are shown. Time is given in seconds since the GRBM trigger. A detailed treatment of GRBM and WFC data can be found in Corsi *et al.* [6].
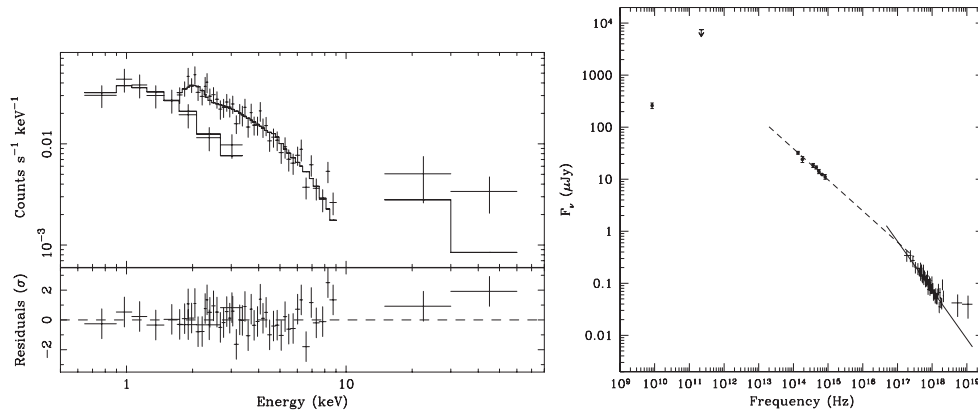
Fig. 2. – Left panel: the 0.6–60 keV afterglow during the first 20 ks of the *BeppoSAX* ToO1. Right panel: SFD at 24.65 Jan. 1999 UT. The optical, NIR and radio data are from Galama *et al.* [10]. As regards the radio data only those acquired strictly within 0.03 d of the reference epoch above are included in the plot. The dashed line is the best-fit power law ($\beta_{\mathrm{opt}} = 0.60$) describing optical and NIR data, the solid line is the power law ($\beta_{\mathrm{X}} = 0.94$) which best fits the *BeppoSAX* NFI data.

The *ASCA* data points acquired after the end of the *BeppoSAX* ToOs are from Yonetoku *et al.* [18]. The host galaxy [3] was subtracted from the R data. Gunn-r magnitudes were converted into R band following Fruchter *et al.* [9]. V and R data were corrected for the Galactic foreground reddening assuming $E(B - V) = 0.016$ [17]. Using a power law model to describe the temporal decay, the 2–10 keV MECS measurements are well fit with an index $\alpha_{\mathrm{X}} = 1.46 \pm 0.04$ (fig. 1, right panel, where the dashed line indicates the best-fit decay of the X-ray afterglow data). We obtained a 2–10 keV light curve from the prompt event to the afterglow, using WFC and MECS data. Moreover, as it is the first time in which an X-ray afterglow is detected above 10 keV, we derived the light curve in the 15–28 keV energy range using WFC data for the prompt emission and PDS data for the afterglow (fig. 1, right panel). The backwards extrapolation of the 2–10 keV power law smoothly reconnects with the late-time WFC data points and upper limits, suggesting that the last WFC points already represent the afterglow emission. Thus, this is the only source for which the Wide Field Cameras have allowed an early detection of the X-ray afterglow between ~ 20 and 60 min after the GRB trigger.

3`2. *Spectra*. – At the beginning of the first ToO the X-ray (0.6–60 keV) afterglow spectrum has a very good statistical quality and for the first time a GRB X-ray afterglow was detected up to 60 keV. A simultaneous combined LECS, MECS and PDS spectrum was obtained in the first 20 ks of the observation, we fitted this spectrum using a photo-electrically absorbed power law with a photon index $\Gamma = 1.94^{+0.12}_{-0.13}$. As the value of N_{H} obtained in this way $(0.9^{+15}_{-0.9} \times 10^{20}\,\mathrm{cm}^{-2})$, is consistent with the Galactic column density along the GRB direction, we fixed its value to the Galactic one $(1.98 \times 10^{20}\,\mathrm{cm}^{-2})$ [7]. The spectra accumulated over the following two time intervals (76.2 ks of ToO1 and the whole ToO2, where the afterglow was detected in the 0.6–10 keV range only) were also analyzed, and the fits were made assuming again a power law description; the best-fit photon index values were found to be completely consistent with that obtained in the first 20 ks spectrum (see table I). Thus we can say that the 3 time resolved spectra are consistent with no spectral variation, *i.e.*, the X-ray afterglow evolution is achromatic.

TABLE I. – *Results of the time-resolved spectral fits of the afterglow BeppoSAX NFI observations. In each case the N_H amount (in squared parentheses) was fixed at the Galactic value. Errors are given at 90% confidence level.*

ToO	Start time (Jan 1999 UT)	Duration (ks)	Γ	N_H (10^{20} cm^{-2})	χ^2/dof
1 (1st part)	23.6495	20	$1.94^{+0.12}_{-0.13}$	[1.98]	40/50
1 (2nd part)	23.8810	76.2	$2.07^{+0.11}_{-0.12}$	[1.98]	56/54
2	24.8132	76.5	$1.86^{+0.29}_{-0.29}$	[1.98]	16/16

3˙3. *Spectral Flux Distribution*. – We considered the Spectral Flux Distribution (SFD) already presented by Galama *et al.* [10] and we completed it with the NFI X-ray data. We referred all data points to date 24.65 Jan 1999 UT. The optical flux densities at the wavelengths of $UBVRIHK$ bands, corrected for the Galactic absorption, have been used without subtracting any host galaxy contribution, because it was negligible at the epoch we selected (cfr. [9]). When needed, we rescaled the data to the corresponding reference date using the optical power law decay with index $\alpha_{\rm opt} = 1.10$ [12]. We rescaled the flux of the broadband X-ray spectrum (0.6–60 keV) using the power law decay measured from 2–10 keV data ($\alpha_{\rm X} = 1.46$). Since the optical and X-ray light curves showed different temporal decays, we independently fitted with a power law the optical/NIR spectrum and we obtained a spectral index value of $\beta_{\rm opt} = 0.60 \pm 0.04$, flatter than the X-ray one ($\beta_{\rm X} = 0.94 \pm 0.07$ at 1σ). The presence of a spectral turnover between optical and X-ray bands could be associated with the change of spectral slope at a frequency which we identified with the cooling frequency ν_c in the framework of the synchrotron fireball model [16]. Assuming a negligible host absorption and using the optical/NIR and X-ray slopes, we obtained for ν_c the value 1.1×10^{17} Hz, corresponding to 0.5 keV.

REFERENCES

[1] AKERLOF C. *et al.*, *Nature*, **398** (1999) 400.
[2] ANDERSEN M. I. *et al.*, *Science*, **283** (1999) 2075.
[3] BLOOM J. S. *et al.*, *ApJ*, **518** (1999) L1.
[4] BOELLA G. *et al.*, *A&AS*, **122** (1997) 299.
[5] CASTRO–TIRADO A. J. *et al.*, *Science*, **283** (1999) 2069.
[6] CORSI A. *et al.*, *A&A*, **438** (2005) 829; see also these proceedings.
[7] DICKEY J. M. and LOCKMAN F. J., *ARA&A*, **28** (1990) 215.
[8] FEROCI M. *et al.*, *IAUC*, **7095** (1999) .
[9] FRUCHTER A. *et al.*, *ApJ*, **519** (1999) L13.
[10] GALAMA T. J. *et al.*, *Nature*, **398** (1999) 394.
[11] JAGER R. *et al.*, *A&AS*, **125** (1997) 557.
[12] KULKARNI S. R. *et al.*, *Nature*, **398** (1999) 389.
[13] MAIORANO E. *et al.*, *A&A*, **438** (2005) 821.
[14] PIRO L. *et al.*, *GCN circ*, **199** (1999) .
[15] PIRO L. *et al.*, *GCN circ*, **203** (1999) .
[16] SARI R. *et al.*, *ApJ*, **497** (1998) L17.
[17] SCHLEGEL D. J. *et al.*, *ApJ*, **500** (1998) 525.
[18] YONETOKU D. J. *et al.*, *PASJ*, **52** (2000) 509.